Role of Magnetic Field Configuration in a Performance of Extended Magnetron Sputtering System with a Cylindrical Cathode

Hui-Gon Chun†, Nikolay S. Sochugov, Yong-Zoo You*, Andrew A. Soloviev**, and Alexander N. Zakharov****

†*School of Materials Science and Engineering, ReMM, University of Ulsan
**Institute of High Current Electronics, Siberian Division of Russian Academy of Science, Tomsk, Russia

ABSTRAT

Extended unbalanced magnetron sputtering system based on the cylindrical magnetron with a rotating cathode was developed. The unbalanced configuration of magnetic field was realized by means of additional lines of permanent magnets, placed along both sides of a 89 mm outer diameter and 600 mm long cylindrical cathode. The performance of the unbalanced magnetron was assessed in terms of the ion current density and the ion-to-atom ratio incident at the substrate. Furthermore, the paper presents the comparison of the internal plasma parameters, such as the electron temperature, electron density, plasma and floating potentials, measured by a Langmuir probe in various positions from the cathode, for conventional and unbalanced constructions of the cylindrical magnetron. The plasma density and ion current density are about 3-5 times higher than those of conventional one, in the unbalanced magnetron in a 0.24 Pa Ar atmosphere with a DC cathode power of 3 kW.

Key Words : Unbalanced magnetron, Permanent magnets, Ion-to-atom ratio, Plasma parameters

1. Introduction

It is known that in 'conventional' or balanced magnetrons the plasma is strongly confined to the target region. A region of dense plasma typically extends about 60 mm from the target surface. Consequently, the ion current drawn at the substrate(usually, <1 mA/cm^2) is generally insufficient to influence the morphological, compositional and crystallizing properties of the films[1]. Thus, it is difficult to deposit fully dense films on large, or complex shape components using balanced magnetrons[2].

To deposit dense films without introducing excessive intrinsic stresses, a high flux(>1 mA/cm^2) of ions is generally preferred[3]. These conditions are readily provided by an unbalanced magnetron. In the unbalanced magnetron the outer lines of magnets are strengthened relative to the inner pole. In this case, not all magnetic field lines are closed between the inner and outer poles in the magnetron, but some are directed toward the substrate. Some secondary electrons are able to follow these field lines and the plasma is no longer strongly confined to the target region but is also allowed to flow out toward the substrate. It was Window and Savvides who first appreciated this effect[4]. They termed this design of the unbalanced magnetron as Type II.

The aim of the present work was to develop the unbalanced magnetron based on a conventional cylindrical magnetron with a rotating cathode and to increase ion current density and ion-to-atom ratio at the substrate. This paper introduces the new design of the unbalanced magnetron comparing its plasma parameters with the parameters of a conventional cylindrical magnetron.

2. Experimental

The magnetron used in the experiments was a conventional cylindrical magnetron with a 89 mm outer diameter and 600 mm long Ti cathode[5]. To obtain unbalanced magnetic fields two additional lines of per-

†E-mail : hgchun@mail.ulsan.ac.kr

manent magnets were placed along both sides of this magnetron in the space between the cathode and substrate. The additional magnets were located at the distance of 150 mm one from another. All magnets were of the same polarity with the internal pole of the magnetron and were electrically insulated from the ground. The magnetic field configurations for the conventional magnetron and the unbalanced magnetron with additional permanent magnets are shown in Fig. 1.

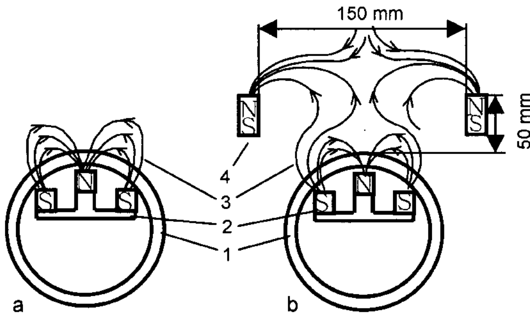

Fig. 1. Diagram of magnetic field configuration in the conventional magnetron (a) and the unbalanced magnetron (b): 1-cathode, 2-magnetron magnetic system, 3-magnetic field lines, 4-additional permanent magnets.

The magnetrons were mounted vertically in a stainless-steel vacuum chamber with the dimensions of 600×600×600 mm^3. The vacuum chamber was equipped by Langmuir probes for plasma measurements. The probes were placed in the centre of the magnetron and were movable in both the vertical and the horizontal directions, as is illustrated schematically in Fig. 2.

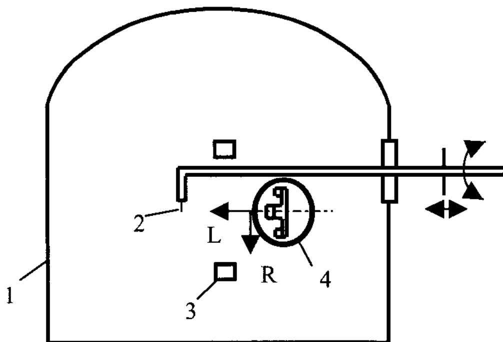

Fig. 2. Schematic diagram of the experimental equipment: 1-vacuum chamber; 2-probe; 3-additional permanent magnets; 4-magnetron; R distance from the magnetron axis; L distance from the cathode.

3. Results and Discussion

Comparison of the magnetic field configurations in the balanced and unbalanced designs of the cylindrical magnetron was carried out with the help of a magnetic induction meter RSH1-10(Russia). In the balanced magnetron most of the field lines emanating from the outer poles converge to the inner pole. A tunnel of field lines is formed between the poles. In the unbalanced magnetron some lines from the outer pole bend over the tunneled region and run parallel to the axis of the magnetron, forming a typical Type II unbalanced field. But a distinctive feature of the magnetron with additional magnets is the presence of two null-points of the magnetic field on the axis of magnetron. The null-point is the region where the vertical component of the magnetic field $B_\perp$ changes its direction on opposite.

Fig. 3 shows the distribution of the vertical component of magnetic field $B_\perp$ measured at various distances L from the cathode on the axis of magnetron (R=0). The component of the magnetic field $B_{//}$ parallel to the cathode was equal to 260 Gs for the balanced magnetron and 280 Gs for the unbalanced one at the distance of 4 mm from the cathode surface.

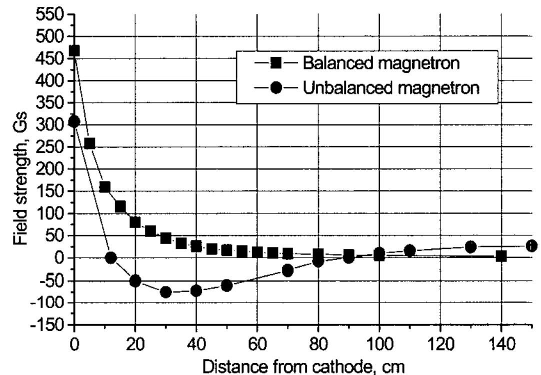

Fig. 3. Distribution of the vertical component of the magnetic field $B_\perp$ at various distances L from the cathode (R=0).

In the balanced magnetron the magnetic field decreases exponentially with increasing the distance from the magnetron surface L and becomes zero at L=145 mm. In the unbalanced magnetron the field lines from the outer poles form the first null-point at L=12 mm. Then $B_\perp$ changes its direction and reaches the maximum of 75 Gs at L=30 mm. The second null-

point is formed at L=90 mm by the field lines from both magnetron magnetic system and additional permanent magnets. At the distances from the magnetron larger than 90 mm, magnetic field is created only by the additional magnets and increased up to 26 Gs at L=150 mm.

The differences in magnetic field configurations of balanced and unbalanced magnetrons result in significant difference in their performance. Fig. 4 presents the distributions of the ion current density J_{ion} and ion-to-atom ratios J_i/J_a incident at the substrate obtained at various distances L from the cathode on the axis of the magnetron(R=0) for both types of the magnetron.

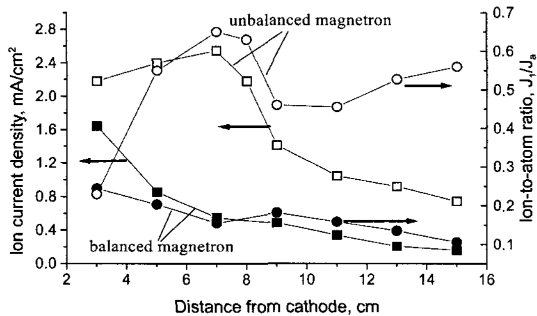

Fig. 4. Distributions of the ion current density Jion and ion-to-atom ratios J_i/J_a incident at the substrate at various distances from the cathode (R=0).

As expected, in the balanced magnetron the ion current density decreased with the distance from the target. It was more than 1 mA/cm^2 only at L<5 cm. Therefore ion-to-atom ratios J_i/J_a incident at the substrate decreased also with the distance from the target from 0.24 to 0.1. The unbalanced magnetron exhibited the increase in 3-5 times both of the ion current density and of the ion-to-atom ratios in comparison with the balanced magnetron. Interestingly, the values of J_{ion} and J_i/J_a are even increased up to L=70 mm. At the distances from the cathode of more than 90 mm they have noticeably smaller values. It is connected with the presense of the second null-point in magnetic field distribution. But it should be noted that, even at L>90 mm, the values of J_{ion} and J_i/J_a are noticeably larger than that in the balanced magnetron. At large distances from the cathode(L>11 cm), the ion-to-atom ratio begins to rise because in this region the deposition rate decreases faster than the ion current density.

Distributions of electron density at different distances from the cathode and at two distances from the magnetron axis (R=0 and R=65 mm) are presented in Fig. 5. In the balanced magnetron, the electron density at both R=0 and R=65 mm gradually decreases with the distance from the cathode from 2.57 to 0.75×10^{10} cm^{-3} and from 2.29 to 0.54×10^{10} cm^{-3}, respectively. In the unbalanced magnetron the electron density is approximately 3-5 times higher in almost all investigated positions. The electron density has maximums of 1.31×10^{11} cm^{-3} at L=50 mm on the axis of magnetron and 5.1×10^{10} cm^{-3} at L=70 mm on the R=65 mm. At large distances from the cathode the difference between the density of electrons on the axis of the magnetron and that on R=65 mm decreases.

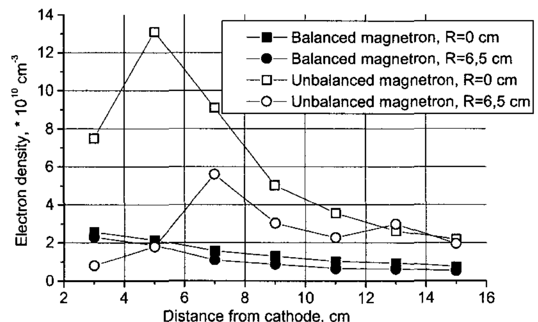

Fig. 5. Distributions of electron density at different distances from the cathode and at two distances from the magnetron axis (R=0 and R=65 mm).

As can be seen in Fig. 6, in the balanced magnetron the plasma and floating potentials weakly changed with the distance from the cathode. The plasma potential was within the limits of 3.5-5.5 V. The difference between the plasma and floating potentials was approximately 8 V and 10 V for R=0 and R=65 mm, respectively. In the unbalanced magnetron the plasma potential is changed within the limits of 0.8-4.8 V. For the floating potential the dependence on the distance from the cathode was revealed on the axis of magnetron. The V_{fl} decreased from -14 V at L=50 mm to -5 V at L=150 mm. Maximum difference between the plasma and floating potentials was observed at L=50 mm and it was equal to 15.5 V. At R=65 mm the difference between V_{pl} and V_{fl} was only 3 V, except for the point at L=70 mm where the difference was 13.5 V.

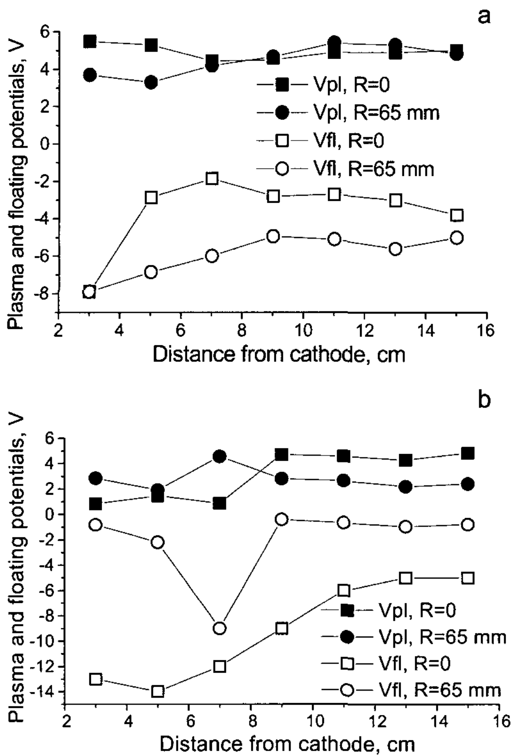

Fig. 6. Distributions of plasma potential V_p and floating potential V_{fl} at different distances from the cathode and at two distances from the magnetron axis (R=0 and R=65 mm).

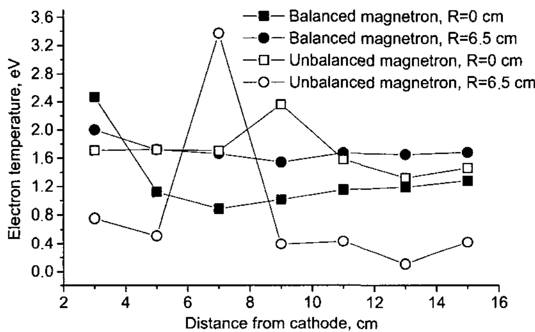

Fig. 7. Distributions of electron temperature Te at different distances from the cathode and at two distances from the magnetron axis (R=0 and R=65 mm) for balanced (a) and unbalanced (b) magnetrons.

The electron temperature in the balanced magnetron weakly changed with the distance from the cathode like the plasma and floating potentials. It has the mean values of 1.1 eV and 1.6 eV for R=0 and R=65 mm, respectively. In the unbalanced magnetron the electron temperature has similar dependence on the distance from the cathode and, on the axis of the magnetron, it changes within the limits from 1.3 to 2.3 eV(Fig. 7). On R=65 mm T_e was very low, varying between 0.1 and 0.75 eV, but at L=70 mm it was abruptly increased up to 2.36 eV. The abrupt increase of all plasma parameters in the region of R=65 mm and L=70 mm is explained by the strong magnetic field in this region due to the immediate vicinity to the additional permanent magnets.

4. Conclusions

The unbalanced magnetron on the basis of a conventional cylindrical magnetron with a rotating cathode has been designed. Two additional lines of permanent magnets placed along both sides of the cylindrical magnetron in the space between the cathode and substrate were used to obtain the unbalanced magnetic field. The distinctive feature of the magnetic field configuration in this magnetron is the presence of the second null-point of the magnetic field on the axis of the magnetron. It has shown that the ion current density and ion-to-atom ratio at the substrate above and below this point are different. However, both the ion current density and the ion-to-atom ratio at the substrate were approximately 3-5 times higher than those in the balanced magnetron in almost all investigated positions. The plasma measurements demonstrated that the electron density is also 3-5 times higher in the unbalanced magnetron in comparison with the balanced one. The principle of performance of this unbalanced magnetron allows to produce extended magnetron sputtering systems with the length up to 2 meters.

Acknowledgements

This work was supported in part by the Korea Science and Engineering Foundation (KOSEF) through the Research Center for Machine Parts and Materials Processing (ReMM) at the University of Ulsan, Korea.

Reference

1. Kelly, P.J. and Arnell, R.D. "Magnetron sputtering: a review of recent developments and applications",

Vacuum, 56, pp. 59-172 (2000).

2. Musil, J. and Kadlec, S. "Reactive sputtering of TiN films at large substrate to target distances", Vacuum, 40, pp. 435-444 (1990).
3. Adibi, F., Petrov, V.J. Greene, E. Hultman, L. and Sundgren, J.E. "Effect of high-flux low-energy (20-100 eV) ion irradiation during deposition on the microstructure and preffered orientation of $Ti_{0.5}Al_{0.5}N$ alloys growth by ultra-high-vacuum reactive magnetron sputtering", J. Appl. Phys, 73, pp. 8580-8589 (1993).
4. Window, B. and Savvides, N. "Charged particle fluxes from planar magnetron sputtering sources", J. Vac. Sci. Technol., A4, pp. 196-202 (1986).
5. Sochugov, N.S. Soloviev, A.A. and Zakharov, A.N. "Cylindrical magnetron sputtering system with a rotating cathode", Proc. of 6th Int. Conf. on Modification of Materials with Particle Beams and Plasma Flows, Russia, Tomsk, pp. 625-628 (2002).
6. Engström, C. Berlind, T. Birch, J. Hultman, L. Ivanov, I. P. Kirkpatrick, S. R. and Rohde, S. "Design, plasma studies, and ion assisted thin film growth in an unbalanced dual target magnetron sputtering system with a solenoid coil", Vacuum, 56, pp. 107-113 (2000).
7. Wiemer, C. Levy, F. and Messier, R. "Effect of ion collisions on Langmuir probe measurements in Ti-N deposition by unbalanced magnetron sputtering", J. Phys. D: Appl. Phys., 29, pp. 99-104 (1996).
8. Laframboise, J.G. and Rubinstein, J. "Theory of a cylindrical probe in a collisionless magnetoplasma", Phys. Fluids, 19, pp. 1900-1908 (1976).